A Solid-State Deuterium NMR Investigation of Conformation and Order in Magnetically Oriented [d(CGCGAATTCGCG)]$_2$†

Todd M. Alam, John Orban, and Gary Drobny*
Department of Chemistry, University of Washington, Seattle, Washington 98195
Received March 9, 1990; Revised Manuscript Received June 22, 1990

ABSTRACT: Solid-state deuterium NMR has been used to investigate the oriented liquid crystal phase of the hydrated oligonucleotide [d(CGCGAATTCGCG)]$_2$. Previous investigations have shown that the helix axis is aligned perpendicular to the magnetic field, while at reduced temperatures motion about the helix axis is eliminated. Synthetic oligonucleotide samples incorporating different labeled nucleosides, [2″-^{2}H]-2′-deoxyadenosine, [*methyl*-^{2}H]thymidine, [8-^{2}H]-2′-deoxyguanosine, and [8-^{2}H]-2′-deoxyadenosine, permitted investigation of both the base and sugar conformation and ordering in the aligned phase. From line-shape analysis of the purine-labeled samples the orientation of the base C8 C–D bond with respect to the helix axis was determined to be $\theta = 90°$ with a distribution of $\sigma_{total} = 20°$, which is comparable to the orientation of $\theta = 90°$, $\sigma_{total} = 15°$, with an oriented fraction $P = 0.7$ found for the C_3 symmetry axis of the methyl-labeled dodecamer. The orientation of the sugar 2″ C–D bond with respect to the helix axis is $\theta = 22°$ with a distribution of $\sigma_{total} = 15°$ in agreement with the expected $C_{2'}$-endo sugar conformation. The fraction of $C_{3'}$-endo was also investigated and from analysis of line shape cannot exceed 20%. These results, though preliminary in nature, illustrate the application of this aligned phase for structural investigations.

The biological importance of structure and dynamics of DNA has been investigated by a number of experimental techniques. With advances in oligonucleotide synthesis, detailed structural information has been obtained by X-ray and 2D NMR[1] studies. X-ray diffraction studies of the B-form *Eco*RI restriction site dodecamer [d(CGCGAATTCGCG)]$_2$ (Wing et al., 1980; Dickerson & Drew, 1981; Dickerson, 1983; Kopka et al., 1983; Privé et al., 1987) suggest that the base orientation varies. Several crystal structures have included a bend in the helix, restricting the assignment of a global helix axis, but have showed an average variation in base roll of $\overline{\theta_R} = 0.24°$ with a standard deviation of $\sigma = 6.8°$ along with an average variation in base tilt of $\overline{\theta_T} = 4.0°$, $\sigma = 3.8°$. Investigation of the reversible bending within the dodecamer and the crystal structure of a straight, undistorted B-form helix (Fratini et al., 1982) allowed the accurate assignment of a global helix axis. Roll and tilt[2] of individual base planes with respect to the global helix axis were obtained with $\overline{\Theta_R} = 8°$, $\sigma = 8°$, and $\overline{\Theta_T} = 3°$, $\sigma = 7°$. In contrast, idealized B-form DNA have roll and tilt values of −3.6° and 0°, respectively (Arnott et al., 1975), and these variations in base orientation differ from the approximately 20° base tilt found in A-form DNA (Saenger, 1984). X-ray crystal data also suggest that the furanose ring tends to adopt a range of conformations from $C_{1'}$-exo to $C_{3'}$-exo. The idealized B-form DNA sugar conformation $C_{2'}$-endo lies in the center of this range, but optimized parameters for B-form conformations (Arnott & Hukins, 1972) suggest that $C_{3'}$-exo may result in more satisfactory refinements. This range of conformations is distinctly removed in the pseudorotation cycle from the $C_{3'}$-endo sugar conformation of A-form DNA.

Solution structures of synthetic oligonucleotides have been investigated by 2D NMR (Reid, 1987), with interproton distances obtained from NOE buildup rates. These distances constitute the basis for structure determination and refinement, utilizing a variety of numerical algorithms including restrained least-squares, distance geometry calculations, and molecular dynamics. For example, the refined distance geometry structure of the dodecamer [d(CGCGAATTCGCG)]$_2$ has recently been reported (Nerdal et al., 1989) and differs from the structure obtained through X-ray investigation. Kinks at the 3–4 and 6–7 steps as well as overall bending of the duplex were observed. Average variation in base roll and tilt were found to be $\overline{\theta_R} = 8.5°$, $\sigma = 14.1°$, and $\overline{\theta_T} = 0.9°$, $\sigma = 1.8°$ (these average values were obtained with only five base-pair steps due to the symmetry of the duplex structure in solution). The sugar conformations fall within essentially the same range of phase angles reported in crystal studies, varying from $O_{4'}$-endo to $C_{3'}$-exo. A recent solution 2D NMR investigation of the dodecamer [d(CGCGAATTCGCG)]$_2$ using homonuclear proton–proton couplings suggests that the sugar conformation is in fast exchange between two conformers. The major conformer falls within a much narrower span than observed in the distance geometry or X-ray structure, ranging from $C_{1'}$-exo to $C_{2'}$-endo. The minor component was restricted to the $C_{3'}$-endo conformation in the analysis, with equilibrium populations as high as 20% (Bax & Lerner, 1988).

Despite significant progress in obtaining structural information on oligonucleotides by X-ray diffraction and high-resolution NMR, the lack of unanimity between these studies suggests that investigation of DNA structure by other techniques would be of value. Solid-state NMR provides a complementary technique for probing biomolecular structure. The majority of work using solid-state NMR has involved studies of oriented peptides and proteins (Cross & Opella, 1985; Nicholson et al., 1987; Stewart et al., 1987; Cornell et al., 1988). By utilization of ^{15}N, ^{13}C, and ^{1}H CSA and dipolar

† This research was supported by NIH Program Project Grant GM 32681-06, NSF Grant DMR8700081, and NIH Molecular Biophysics Grant GM 08268-02 to T.M.A.

[1] Abbreviations: 2D NMR, two-dimensional NMR spectroscopy; NMR, nuclear magnetic resonance; EFG, electrical field gradient; PAS, principal axis system; *P*, oriented fraction.

[2] The angle between the C–D bond and the global helix axis is denoted as θ. With this convention, the commonly utilized base tilt Θ_T is equal to $90° - \theta$.

0006-2960/90/0429-9610$02.50/0

interactions along with the ^2H quadrupolar interaction, the peptide backbone configurations of several oriented proteins and polypeptides have been determined. In contrast to solution studies, structural information from solid-state NMR is obtained in terms of angles instead of distances (Brenneman & Cross, 1990). Studies of oriented DNA fibers (Nall et al., 1981; Shindo et al., 1985) and virus DNA (Cross et al., 1983) by ^{31}P NMR has allowed structural information about the phosphorus backbone to be determined. Investigation of the sugar pucker in DNA by solid-state ^{13}C NMR confirms that the major conformation is $C_{3'}$-endo for A-DNA and $C_{2'}$-endo for B-DNA (Santos et al., 1989). One nuclear interaction that has not received extensive use as a structural probe is the quadrupolar interaction in deuterium NMR.

Solid-state ^2H NMR has been used primarily to elucidate the base dynamics of polynucleotides (DiVerdi & Opella, 1981; Bendel et al., 1983; James et al., 1983; Vold et al., 1986; Brandes et al., 1986, 1988a,b; Shindo et al., 1987). Recent investigations of dynamics in synthetic oligonucleotides using ^2H NMR have included site-selective deuteration, which allows the study of base dynamics (Kintanar et al., 1989), methyl group dynamics (Alam & Drobny, 1990a), and furanose ring dynamics (Huang et al., 1990) in $[d(CGCGAATTCGCG)]_2$. Studies of internal motions within the sugar ring of the nucleosides 2′-deoxyguanosine and thymidine have also been reported (Roy et al., 1986; Hiyama et al., 1989). Investigation of structural questions in DNA by ^2H NMR has been limited to characterization of purine base tilt and order in oriented DNA films and fibers (Vold et al., 1986; Shindo et al., 1987; Brandes et al., 1988a,b). The fiber investigation by Shindo and co-workers found that the base tilt was $\sim 20°$ for A-form DNA and $\sim 0° \pm 10°$ for B-form DNA. Investigation of oriented Li-DNA by Brandes and co-workers found the average base roll $\overline{\Theta_R} \sim 0°$ with $\sigma = 9°$ for the B-form DNA at $\mathbf{W} \sim 10$ (mol of H_2O/mol of nucleotide), while Na-DNA in the A-form ($\mathbf{W} = 8.6$) resulted in $\overline{\Theta_R} \sim 23°$ and $\sigma \sim 4°$. The static order was also investigated with changes in $\mathbf{W}$ for oriented Li-DNA and was found to decrease from $\sigma = 17°$ at $\mathbf{W} = 0.5$ to $\sigma = 9°$ for $\mathbf{W} = 6$ through $\mathbf{W} = 13.4$.

Liquid crystal phases have been observed for concentrated solutions of DNA (Robinson, 1961; Iizuka, 1977, 1978, 1983; Rill et al., 1983; Rill, 1986), including the synthetic dodecamer $[d(CGCGAATTCGCG)]_2$ (Alam & Drobny, 1990a). Preliminary ^2H NMR investigation of the oriented phase and dynamics using the [*methyl*-^2H]thymidine-labeled dodecamer have been reported (Alam & Drobny, 1990b). The liquid crystal phase was found to exist for dodecamer concentrations ranging from 490 to 722 mg mL^{-1}, with the helix axis aligning perpendicular to the magnetic field. We report a structural investigation of the selectively deuterated synthetic oligonucleotide $[d(CGCGAATTCGCG)]_2$ in the liquid crystal phase. Three different samples containing the labeled nucleosides ([*methyl*-^2H]thymidine, $[d(CGCGAAT*T*CGCG)]_2$; [8-^2H]-2′-deoxyadenosine and [8-^2H]-2′-deoxyguanosine, $[d(CG*CG*A*A*TTCG*CG*)]_2$; [2″-$^2H$]-2′-deoxyadenosine, $[d(CGCGA*A*TTCGCG)]_2$) were investigated. By analysis of line shapes obtained at reduced temperatures for these highly hydrated samples, information concerning the base and sugar conformation and order were obtained.

Materials and Methods

Labeled Synthesis. Preparation of the various labeled dodecamers involved introducing the specifically labeled phosphoramidite at the appropriate step in the synthesis. Synthesis of [*methyl*-^2H]thymidine (Kintanar et al., 1988; Alam & Drobny, 1990a), [2″-^2H]-2′-deoxyadenosine (Huang et al., 1990), and [8-^2H]-2′-deoxyguanosine (Kintanar et al., 1989) and purification of the respectively labeled oligonucleotides have been previously described. To the purified, desalted DNA was added 10% NaCl by weight, followed by lyophilization from ^2H-depleted water, resulting in 56.5 mg of the methyl-labeled dodecamer, 41.4 mg of the sugar-labeled sample, and 33.3 mg of the nonselective purine labeled dodecamer. The samples were hydrated over appropriate salt solutions with ^2H-depleted water. Water adsorption was monitored gravimetrically, allowing the determination of $\mathbf{W}$ (mol of H_2O/mol of nucleotide). These results are presented in Table I. Some variation in water content for a given relative humidity has been noted previously (Alam & Drobny, 1990b).

Table I: Experimental Parameters for Magnetically Oriented $[d(CGCGAATTCGCG)]_2$[a]

	A	B	C
$\mathbf{W}(H_2O$/nucleotide)	29.6	30.5	28.9
concn (mg/mL)	654	635	685
temp (K)	228 ± 3	200 ± 3	200 ± 3
$\bar{\theta}$ (deg)	90 ± 10	90 ± 10	22 ± 3
σ_{total} (deg)	15	20	15
P	0.7	0.7	0.7

[a] A = [*methyl*-^2H]thymidine-labeled $[d(CGCGAAT*T*CGCG)]_2$. B = [8-^2H]purine-labeled $[d(CG*CG*A*A*TTCG*CG*)]_2$. C = [2″-$^2H$]-2′-deoxyadenosine-labeled $[d(CGCGA*A*TTCGCG)]_2$.

Solid-State NMR Spectroscopy. Solid-state ^2H NMR spectra were obtained at 76.75 MHz with an eight-step phase-cycled quadrupolar echo sequence, $\pi/2_x-\tau_1-\pi/2_{\pm y}-\tau_2-$acq (Griffin, 1981). The $\pi/2$ pulse length was ≤ 2.5 μs for the methyl-labeled sample and ≤ 2.3 μs for the sugar- and base-labeled samples. The pulse spacing τ_1 was 50 μs, while data acquisition was initiated prior to the solid echo by adjustment of τ_2. The recycle delay was at least 5 times the T_1 observed in the dry samples, since the T_1 was not determined for the frozen liquid crystal phase. The number of acquisitions varied from 8000 to 24 000 scans. Lorentzian line broadening of 500–1000 Hz for the methyl-labeled sample and 5000 Hz for the sugar-labeled and nonselective base labeled sample was applied to experimental spectra to obtain adequate signal to noise. Temperature was controlled with liquid N_2 boil off and was constant within ±3 deg; experimental temperatures are given in Table I.

Line-Shape Simulations. Simulations of deuterium line shapes were obtained with the program MXQET, which can accommodate multisite, multiaxis motional models, along with finite-pulse corrections. MXQET has been described in detail elsewhere (Greenfield et al., 1987). A modified version, GNMXQET, allowing different distributions of the helix axis orientation, was used to simulate the aligned spectra. Static values of the quadrupolar coupling constant (e^2qQ/h) and the asymmetry parameter (η) were obtained from previous investigations (Tsang et al., 1987; Kintanar et al., 1988, 1989; Huang et al., 1990). Values of the standard deviation (σ) and oriented fraction (P) were obtained from best visual fits to experimental line shapes. All simulations were run on a DEC Vaxstation 3200.

Analysis of Quadrupolar Line Shapes. For an isolated deuteron in a solid, the NMR frequency is given by

$$\omega = \omega_0 \pm \omega_Q \tag{1a}$$

where

$$\omega_Q = (3\pi/4)\frac{e^2qQ}{h}[3\cos^2\Theta - 1 - \eta\sin^2\Theta\cos 2\Phi] \tag{1b}$$

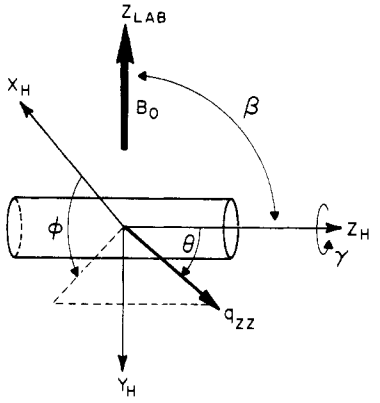

FIGURE 1: Illustration of coordinate system for a uniaxial EFG tensor. The orientation of the q_{zz} component of the EFG tensor with respect to the intermediate helix axis frame is described by the angles θ and ϕ. The orientation of the helix frame with repect to the external magnetic field $\mathbf{B}_0$ is described by β and γ.

e^2qQ/h is the quadrupolar coupling constant (QCC) and η is the asymmetry parameter which describes the deviation from cylindrical symmetry of the electrical field gradient (EFG) tensor about the q_{zz} axis in the principal axis system (PAS). The orientation of the magnetic field $\mathbf{B}_0$ in the PAS of the EFG is described by the polar angles Θ and Φ (Abragam, 1961). To quantitatively describe the effects of helix alignment on the resonant frequency, it is convenient to introduce an intermediate helix frame of reference. Transformation between these frames by use of the simplifying assumption of a symmetric EFG tensor results in

$$\omega_Q = (3\pi/2)\frac{e^2qQ}{h}[P_2(\cos\theta)P_2(\cos\beta) - (3/4)\sin 2\theta \sin 2\beta \cos(\gamma + \phi) + (3/4)\sin^2\theta \sin^2\beta \cos 2(\gamma + \phi)] \quad (2)$$

where $P_2(x)$ are second-order Legendre polynomials. The angles θ and ϕ define the orientation of the EFG tensor in the helix axis frame, and the angles β and γ describe the orientation of the helix axis with respect to the laboratory frame. A visual representation of these frames is shown in Figure 1. In particular, β describes the angle between the helix axis and the magnetic field, γ describes the relative rotation about the helix axis, and θ describes the angle between the C–D bond and the helix axis (making the assumption that the q_{zz} tensor element is coincident with the C–D bond) while ϕ describes the orientation of the bond about the helix axis. Since γ and ϕ commute, ϕ can be set to zero without loss of generality. For a non-zero asymmetry parameter, an additional angle χ is required to describe the orientation of the EFG tensor in the helix axis frame; ω_Q then becomes dependent on the asymmetry parameter. Internal motions also affect the observed quadrupolar frequency: anisotropic base motion modeled as restricted diffusion in two perpendicular planes (Brandes et al., 1988a,b) along with the analogous effect on the methyl group frequency (Alam & Drobny, 1990b) have been reported in the literature.

If the helix axis does not align perfectly in the magnetic field, there will be a distribution of β angles. Simulations of the experimental line shapes were obtained with appropriate weighting of β characterized by an orientational function $f(\beta)$ (Luz et al., 1981; Alam & Drobny, 1990b):

$$I(\omega) = \int\int I(\omega,\beta,\gamma,\theta,\phi)f(\beta)\sin(\beta)\,d\beta\,d\gamma \quad (3)$$

Different forms of $f(\beta)$ are available, but experimental spectra were simulated by superimposing domains where the helix axis is randomly oriented with domains where the helix axis is highly ordered. A Gaussian distribution was assumed for the oriented domains, the functional form of $f(\beta)$ being given by

$$f(\beta) = (P/\sigma\sqrt{2\pi})e^{-(\beta-\beta_0)^2/2\sigma^2} + (1 - P) \quad (4)$$

where P is the fraction of the sample in the oriented domain, β_0 is the mean angle of alignment, and σ is the standard deviation in the Gaussian distribution. Variation in the line shape with changes in these parameters has been discussed previously (Brandes et al., 1988a,b; Alam & Drobny, 1990b).

Results and Discussion

Characteristics of the Aligned Phase. Proof of alignment is demonstrated by the spectra shown in Figure 2. Figure 2A shows the [*methyl*-^{2}H]thymidine-labeled dodecamer at a reduced water content [**W** = 16.8 (mol of H_2O/mol of nucleotide)] which was frozen inside the magnetic field. This level of hydration was not observed to form an oriented phase during the time scale of previous investigations (24–48 h). The spectrum is characteristic of an unoriented sample, differing significantly from the experimental line shape shown in Figure 3B, suggesting that the unique features are not a result of obtaining the spectra at reduced temperatures. Figure 2B shows the result of rotating the frozen, aligned [*methyl*-^{2}H]thymidine-labeled sample about the X or Y laboratory axis. The spectrum demonstrates that there is helix ordering with respect to the angle β, but no macroscopic order is present about α (around B_0). This is clear if one imagines that all the dodecamer helix axes align perpendicular to the field (β = 90°), but within the plane defined by the β = 90° angle there is no macroscopic order (no order in α). When the sample is rotated about a laboratory X or Y axis, the helix axes now have a range of β values eliminating the characteristic cylindrical line shape observed for the oriented sample. Freezing samples outside the magnetic field prevents alignment of the dodecamer when placed within the field. The result is a line shape characteristic of an unoriented sample as shown in Figure 2C.

Investigation of Conformation and Order. From the discussion of the analysis of ^{2}H line shapes, the orientation of the C–D bond with respect to the helix axis can be determined. The oligonucleotide in the liquid crystal phase has uniaxial order; therefore, only θ, β_0, and σ can be determined. The ^{2}H NMR spectra of [*methyl*-^{2}H]thymidine-labeled [d(CGCGAAT*T*CGCG)]$_2$, [8-^{2}H]-2′-deoxyadenosine-labeled and [8-^{2}H]-2′-deoxyguanosine-labeled [d(CG*CG*A*A*TTCG*CG*)]$_2$, and [2″-^{2}H]-2′-deoxyadenosine-labeled [d(CGCGA*A*TTCGCG)]$_2$ are shown in Figure 3A,B and Figure 6A. The water content **W**, concentration, and experimental temperatures are given in Table I. At reduced temperature the observed line shapes are characteristic of aligned samples. Use of reduced temperatures is critical to obtain line shapes that are not highly averaged by motion about the helix axis. Examples of this motional averaging have been presented previously (Alam & Drobny, 1990b). Librational amplitudes were not determined in the nonselectively base-labeled or sugar-labeled material due to insufficient signal to noise. Spin–lattice relaxation times (T_1) and quadrupolar echo decay times (T_{2e}) were determined only for [*methyl*-^{2}H]thymidine-labeled [d(CGCGAAT*T*CGCG)]$_2$ and have been reported in the original characterization of the liquid crystal phase (Alam & Drobny, 1990b).

Base Orientation and Order. From the spectra of the methyl- and base-labeled material, information concerning the conformation and order within the base domain is obtained.

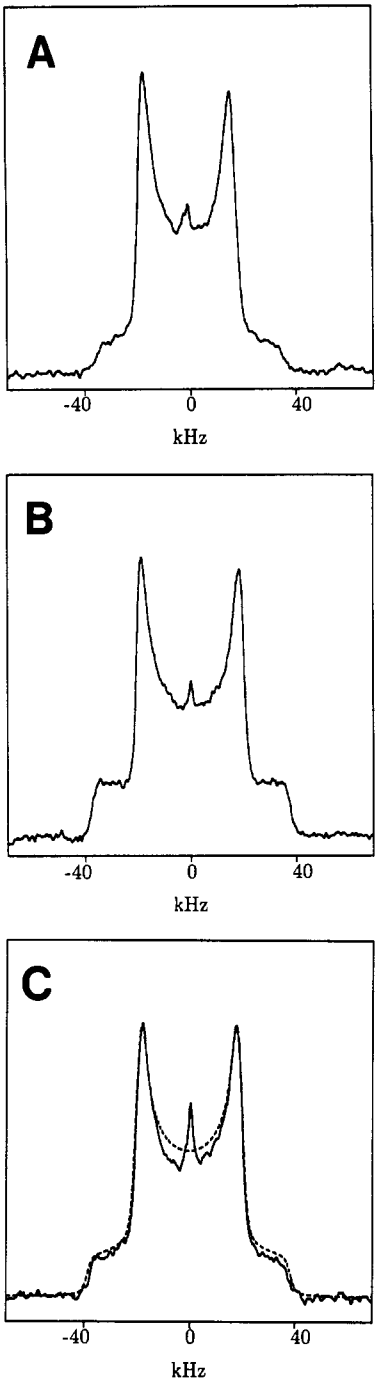

FIGURE 2: (A) Experimental spectrum of [*methyl*-^{2}H]thymidine-labeled [d(CGCGAAT*T*CGCG)]$_2$ using 12 000 scans, $\pi/2$ = 2.3 μs, and W = 16.8; representative of an unaligned sample. (B) Spectrum of [*methyl*-^{2}H]thymidine-labeled [d-(CGCGAAT*T*CGCG)]$_2$ using 8000 scans, $\pi/2$ = 2.5 μs, and W = 29.6; frozen while aligned in field (see Figure 3B) and then rotated about the X_{lab} axis. (C) Experimental (—) and simulated (---) spectra of labeled [d(CGCGAATTCGCG)]$_2$ using 8400 scans, $\pi/2$ = 2.4 μs, and W = 30.0; frozen while outside the magnet, representing an unaligned sample.

The effects of the variables σ, β_o, θ, and P on the line shape of the purine base labeled material are shown in Figure 4. Similar effects were investigated for the [*methyl*-^{2}H]thymidine-labeled dodecamer (Alam & Drobny, 1990b). Finite pulse effects are less pronounced in the methyl-labeled spectra due to the reduced line width resulting from the rapid 3-fold jump of the methyl group.

The spectrum of nonselectively [8-^{2}H]-2′-deoxyguanosine-labeled and [8-^{2}H]-2′-deoxyadenosine-labeled [d-(CG*CG*A*A*TTCG*CG*)]$_2$ was simulated with QCC_{eff} = 178 kHz, η_{eff} = 0.08, θ = 90°, σ = 20°, and P = 0.7 (Figure 3A). By use of these effective values the $\overline{q_{xx}}$ element of the averaged EFG tensor lies approximately within the base plane (χ = 90°), in agreement with that observed by Brandes et al. (1988a). The random fraction value was determined from the methyl-labeled spectrum, which has much higher signal to noise. The values of QCC_{eff} and η_{eff} are the same as observed in the dry dodecamer. If one uses the static values of QCC_{static} = 179 kHz and η_{static} = 0.06, the observed effective values would require an additional libration in two orthogonal planes of ca. ±7° and ca. ±2° (Kintanar et al., 1989). Unlike the investigation of the methyl-labeled dodecamer, the signal to noise of the purine-labeled material does not allow a distinction to be made between the effects of tilting and twisting librations on the line shape. The simulation parameters listed in Table I for the nonselectively purine labeled sample assumed that the experimental spectra can be described by a single average θ and σ_{total} (see later discussion). The experimental spectra could also be simulated by use of average θ values ranging from 80° to 100° with only small changes in σ. Base tilt angles exceeding this range produced simulations different from experimental data (see Figure 4C). Similarly, variation of the standard deviation σ also produced line shapes not observed experimentally (see Figure 4A). From previous investigations of the [*methyl*-^{2}H]thymidine-labeled dodecamer, the spectrum was simulated with θ = 90°, σ = 15°, P = 0.7, QCC_{static} = 159 kHz, η_{static} = 0, and a rapid 3-fold jump about the C_3

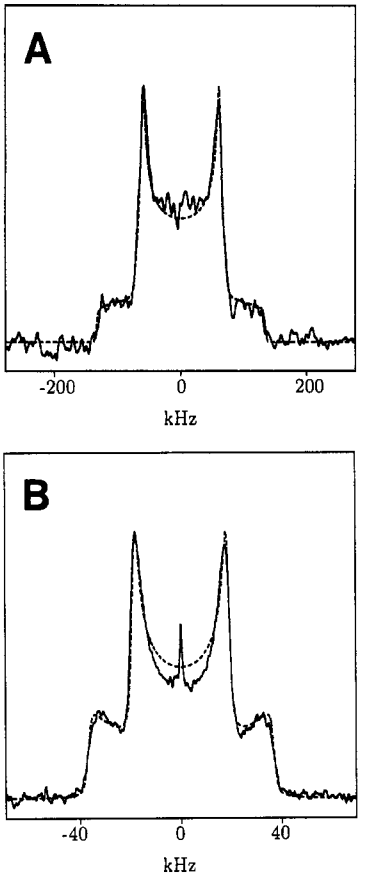

FIGURE 3: Experimental (—) and simulated (---) 76.75-MHz deuterium quadrupole echo spectra of labeled [d(CGCGAATTCGCG)]$_2$ in the oriented liquid crystal phase. The simulated spectra were calculated as described in the text; the central isotropic component being ignored. By use of a pulse delay of 50 μs, spectra were obtained for (A) [8-^{2}H]purine-labeled [d(CG*CG*A*A*TTCG*CG*)]$_2$ (13 000 scans, $\pi/2$ = 2.3 μs, W = 27.7) and (B) [*methyl*-^{2}H]thymidine-labeled [d(CGCGATT*T*CGCG)]$_2$ (8000 scans, $\pi/2$ = 2.5 μs, W = 29.6).

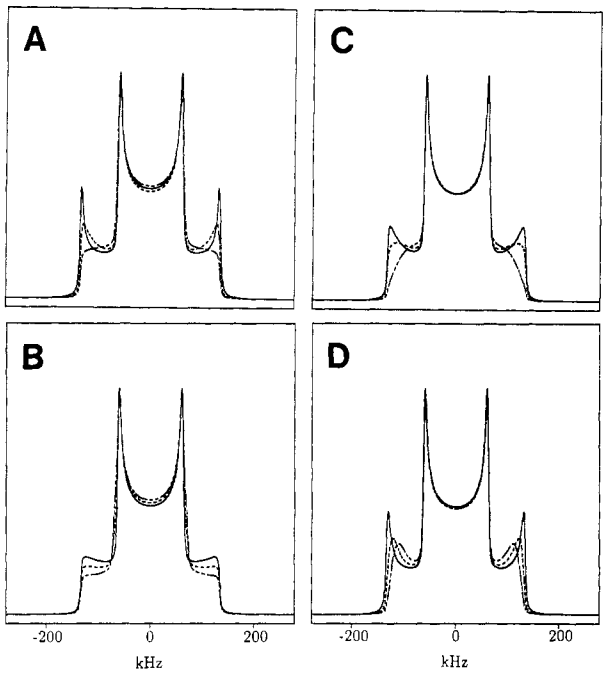

FIGURE 4: Simulated quadrupole echo spectra as a function of Gaussian distribution parameters. (A) Variation in σ_{total}: (—) 1°; (---) 10°; (----) 20°. $\beta_o = 90°$; $\theta = 90°$; $P = 1.0$. (B) Variation in P: (—) 1.00; (---) 0.75; (----) 0.50. $\beta_o = 90°$; $\theta = 90°$; $\sigma_{total} = 15°$. (C) Variation in θ: (—) 90°; (---) 80°; (----) 70°. $\beta_o = 90°$; $P = 1.0$; $\sigma_{total} = 10°$. (D) Variation in β_o: (—) 90°; (---) 80°; (----) 75°. $\theta = 90°$; $P = 1.0$; $\sigma_{total} = 5°$.

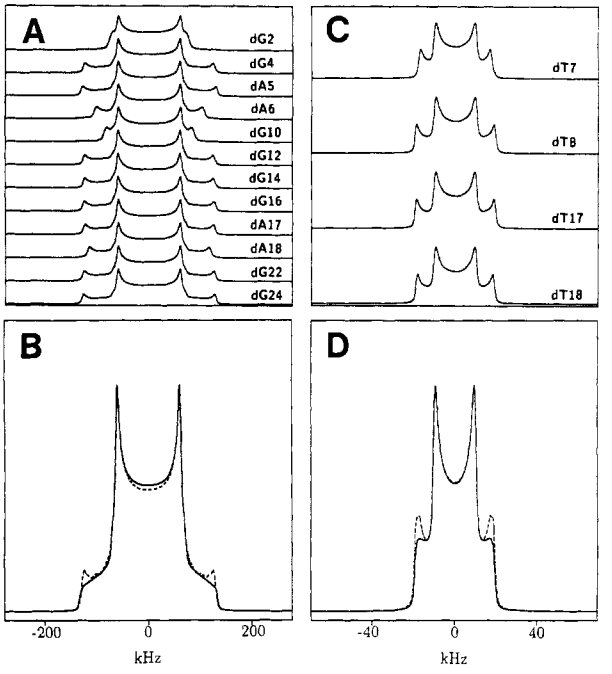

FIGURE 5: Simulated spectra using the solution NMR distance geometry structure. (A) Individual spectrum for nonselective purine labeled dodecamer; $\sigma_\beta = 1°$. (B) Sum of individual spectrum: (—) $\sigma_\beta = 15°$; (---) $\sigma_\beta = 1°$. (C) Individual spectrum for [*methyl*-^{2}H]thymidine, $\sigma_\beta = 1°$. (D) Sum of individual spectrum: (—) $\sigma_\beta = 15°$; (---) $\sigma_\beta = 1°$.

symmetry axis of the methyl group, along with a tilt libration $\theta_o = 10° \pm 3°$ and a twisting libration of $\phi_o = 15° \pm 3°$ (see Figure 3B). Since the C–D vector of the [8-^{2}H]purine is ~15° from the roll axis, to a first approximation base roll and propeller twist will have a small effect on the ^{2}H NMR powder pattern. In contrast, the C_3 symmetry axis of the methyl group is ~72° from the roll axis so that the angle θ with respect to the helix axis is affected by both roll and twist. Therefore, the θ distribution found in the base- and methyl-labeled material cannot be directly compared. As pointed out by Brandes et al. (1988a), it is not possible to distinguish between a helix distribution σ_β and a distribution in the orientational angle σ_θ. If one assumes that these distributions are independent, the standard deviation of the Gaussian distribution determined experimentally is described by σ_{total}, where

$$\sigma_{total}^2 = \sigma_\beta^2 + \sigma_\theta^2 \quad (5)$$

If the purine- and methyl-labeled samples have the same distribution of β, the largest possible σ_β is 15° (i.e., the σ_{total} of the methyl-labeled sample, assuming $\sigma_\theta = 0°$). The minimum θ distribution for the nonselective labeled purine is therefore $\sigma_\theta \sim 13°$ from relation 5.

These values of the angle θ and the standard deviation σ_θ can be compared to those from previous structural studies and are similar to the values obtained from X-ray investigations (Fratini et al., 1982). Since only tilt magnitude is measured in our investigations, the average tilt magnitude $\overline{|\Theta_T|}$ and distribution $\sigma_{|\Theta_T|}$ corresponding to the crystal structure were determined. For the purine bases this is $\overline{|\Theta_T|} = 4.3°$ (i.e., $\theta = 85.7°$) and $\sigma_{|\Theta_T|} = 3.1°$, while the average tilt magnitude for the thymidines is $\overline{|\Theta_T|} = 9.3°$ and $\sigma_{|\Theta_T|} = 1.0°$. Recall that there will be a small contribution from the roll to the apparent tilt values for the purine-labeled material and a larger contribution to the apparent tilt for the methyl-labeled material: these contributions were not calculated. The portion of σ_{total} for the methyl-labeled sample that results from variation in base tilt cannot be determined without additional labeled samples to determine σ_β. The average tilt value determined from X-ray structural data does not conflict with what is observed experimentally, but the crystal structure shows a significantly lower distribution in $\overline{|\Theta_T|}$ than the minimum θ distribution possible in the purine sample.

Comparison to the distance geometry liquid structure (Nerdal et al., 1990) is also possible. Because the solution structure shows steps at 3–4 and 6–7, a global helix axis cannot be identified. However, by use of the $(AATT)_2$ tract to define a "local" helix axis, which is assumed to be oriented approximately perpendicular to the magnetic field, tilt angles relative to this local axis can be determined. Because this axis does not coincide with the 2-fold symmetry axis of the molecule, the θ angles are nonequivalent for 2-fold symmetry related nucleotides. The assumption that the "local" axis is aligned approximately perpendicular to the magnetic field is justified from analysis of the distinct cylindrical line shape observed for the [*methyl*-^{2}H]thymidine-labeled material (see Figure 3B). The average magnitude of tilt from this local helix axis for the purines is found to be $\overline{|\Theta|} \sim 15°$ with $\sigma_{|\Theta|} \sim 9°$. The average tilt value is slightly larger than the range observed experimentally, but the Θ distribution is the same as the minimum θ distribution observed experimentally. Simulations of each purine base and associated tilt angle are given in Figure 5A (the first strand is numbered 1–12 and the second 13–24). This figure shows the variation in line shape theoretically observable for a nonselectively labeled dodecamer. Unfortunately, it is the sum of the individual spectra that is obtained experimentally. The additional loss of information due to the distribution in the helix alignment, σ_β, is portrayed in Figure 5B. Increasing the helix axis alignment distribution tends to further obscure structural information, where at high σ_β the spectra converge to simulations obtained with average $\overline{|\Theta|}$ and $\sigma_{|\Theta|}$. Thus for larger helix distributions, mean values of θ are

sufficient to describe the base conformation. Comparison of the experimental spectra with these simulations suggests that σ_β is probably less than 15°, the remaining distribution residing in θ. Figure 5 also illuminates a major weakness of using nonselectively labeled materials for conformational studies. More detailed information could be obtained from several samples with different sites selectively labeled. Such work is in progress. Inspection of Figure 5A predicts radically different line shapes for purines that reside on opposite sides of the steps at 3–4 and 6–7 (for example, compare G2 and G4). Selectively labeled samples may allow direct observation of these kinks. Similar investigation for the tilt of the C_3 axis of the methyl group for the thymidines gives $\overline{|\Theta|} \sim 6°$ and $\sigma_{|\Theta|} \sim 6°$. This average Θ value is within the range observed experimentally. If one assumes that $\sigma_\theta = 6°$ for the methyl-labeled sample, the use of relation 5 gives the reduce helix distribution $\sigma_\beta = 13.7°$. The minimum θ distribution for the purine base labeled material is then $\sigma_\theta = 14.5°$. Simulation of individual methyl line shapes is shown in Figure 5C, showing very similar line shapes for all the thymidines in the dodecamer. The effects of σ_β on additive spectra of the thymidines are shown in Figure 5D. The simulation for $\sigma_\beta = 15°$ is in close agreement with the experimental spectrum.

Sugar Conformation. The analysis of sugar conformation proceeds in a similar fashion. By utilizing the maximum σ_β possible (i.e., $\sigma_\beta = 15°$), $QCC_{eff} = 174$ kHz, $\eta_{eff} = 0.03$, and $P = 0.7$, the angle between the helix axis and the C–D bond of the C2″ position is $\theta = 22°$ (see Figure 6A). The contributions from the approximately 10% deuterium label present at the 2′ position were ignored; this omission results in a slightly increased value of θ. Using $\sigma_\beta = 15°$ means that there is no distribution in θ. As in the previous discussion, using the value of $\sigma_\beta = 13.7°$ and relation 5 gives $\sigma_\theta = 6.1°$. Decreasing the β distribution would require an increase in the value of θ, but for values of $\theta \geq 25°$ (see Figure 6B) simulations did not reproduce the experimental line shape. These simulations were obtained with an average θ value to describe the sugar conformation, an assumption that may not be realistic considering the average involves only four 2′-deoxyadenosines (see discussion below). This range of θ values (20–25°) corresponds well to the value of $\theta = 22.5°$ expected for the $C_{2'}$-endo configuration in model B-form DNA. As a comparison the $C_{3'}$-endo sugar conformation of A-form DNA results in the 2″ C–D bond having a θ angle of approximately 90°. Simulations for this large θ do not reproduce the experimental spectra (see Figure 6A).

These results can also be compared to the sugar conformation observed in previous structural investigations. Considering only the 2′-deoxyadenosine sugar conformations in the crystal structure of the dodecamer, one obtains $|\bar{\Theta}| = 42.7°$ with $\sigma_{|\Theta|} = 14°$. Both of these values differ significantly from the θ observed experimentally. Comparison to the distance geometry solution structure (using the same assumptions about local helix axis as the base investigation) results in $|\bar{\Theta}| = 42°$ with $\sigma_{|\Theta|} = 29°$. Again, the average Θ value and deviation are significantly larger than the values observed experimentally and are similar in magnitude to those observed in the crystal structure. Simulations for each of the C2″ of 2′-deoxyadenosines and associated Θ value are shown in Figure 6C, while the sum for $\sigma = 15°$ and $\sigma = 1°$ is shown in Figure 6D. The sum of these simulations for $\sigma = 15°$ has additional center intensity in comparison to experimental spectra, while the simulations using $\sigma = 1°$ have fine structure that is not observed experimentally. Obviously, an average θ value does not converge to the sum of spectra for low numbers of sites, in contrast to the case observed in the purihe-labeled sample.

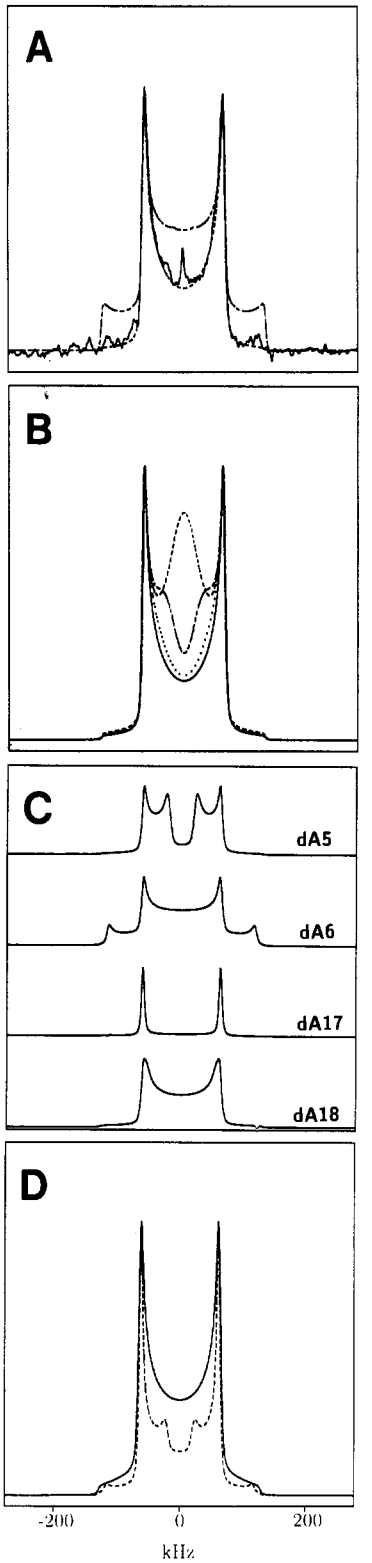

FIGURE 6: (A) Experimental (—) spectrum of [2″-^2H]-2′-deoxyadenosine-labeled [d(CGCGA*T*TTCGCG)]$_2$ using 24 340 scans, $\pi/2 = 2.3$ μs, and $W = 28.3$; simulated (---) spectrum for $C_{2'}$-endo sugar conformation in model B-form DNA; simulated (–---) spectrum for $C_{3'}$-endo configuration of model A-form DNA. (B) Variation in θ: (—) $\theta = 20°$, $\sigma_\beta = 15°$; (····) $\theta = 25°$, $\sigma_\beta = 10°$; (–---) $\theta = 30°$, $\sigma_\beta = 5°$; (---) $\theta = 35°$, $\sigma_\beta = 5°$. (C) Simulated spectra using solution NMR distance geometry structure for each of the 2″-labeled adenosines in the dodecamer. (D) Sum of individual simulations for (—) $\sigma_\beta = 15°$ and (---) $\sigma_\beta = 1°$.

The possibility of sugar conformer mixtures was also investigated. Recent ^2H solid-state NMR studies of internal

dynamics in the furanose ring of [d(CGCGAATTCGCG)]$_2$ suggest that fast, large-amplitude motions such as interconversion between $C_{2'}$-endo and $C_{3'}$-endo do not occur on the nanosecond time scale (Huang et al., 1990). Unfortunately, the analysis of ^{2}H NMR quandrupolar echo line shapes is insensitive to motions occurring at rates slower than 10^4 Hz and in any case may not be able to detect small populations of $C_{3'}$-endo. In contrast, investigation of sugar conformations within the dodecamer by analysis of coupling constants suggests that there is rapid interconversion between two conformers (Bax & Lerner, 1988), with the $C_{3'}$-endo population of the 2′-deoxyadenosines calculated to be 6–7%. Simulations of mixtures between $\theta = 22°$ ($C_{2'}$-endo) and $\theta = 90°$ ($C_{3'}$-endo, A form) suggest the maximum mixture that would fit the experimental data was ~20% for the $\theta = 90°$ conformer. This value must be approached with caution since the θ value used for the $C_{3'}$-endo configuration was obtained from model A-form DNA. The conformation of the sugar cannot be obtained with only the 2″-labeled material. It will become necessary to utilize labels at additional positions to determine the complete sugar conformation.

Conclusions

We have shown that the oriented liquid crystal phase formed by oligonucleotides at high hydration levels can be utilized to investigate molecular structure and order by solid-state ^{2}H NMR. The base orientation and sugar conformation have been investigated with the deuterated dodecamer [d(CGCGAATTCGCG)]$_2$. The loss of structural information accompanying the use of nonselectively labeled samples necessitates that selectively deuterated oligonucleotides be produced. Although selective deuteration is laborious, ^{2}H provides a complementary technique to probe the local structure of oligonucleotides currently under study by X-ray and high-resolution NMR methods. One advantage of solid-state NMR is that the growth of a diffractable crystal is not required. If selectively deuterated samples are prepared, solid-state NMR methods are free of the necessity of performing assignments of nuclear resonances, as is required by 2D NMR methods, so virtually any oligonucleotide sequence that produces a phase with an identifiable ordering axis can be investigated. In addition, the size of oligonucleotides that can be studied is limited only by the practical yield in the DNA synthetic protocols, and we anticipate the ability to study sequences up to 40–50 base pairs in the near future. The liquid crystalline phase of oligonucleotides is lyotropic and only exists at relatively high levels of hydration. However, phase ordering is preserved at reduced temperatures, where large-amplitude microsecond time scale motions about the helix axis are effectively quenched. Ordering also occurs at easily available field strengths; for instance, the methyl-labeled dodecamer was aligned at only 4.5 T. In summary, solid-state NMR methods are capable of yielding structural information in addition to the internal dynamics of oligonucleotides. The conformation and structure of the base domains in [d(CGCGAATTCGCG)]$_2$ agree well with the distance geometry solution structure. In contrast, the agreement between $\overline{|\theta|}$ of the 2″ orientation and either the X-ray or distance geometry solution structure is poor. The conformation of furanose rings cannot be exactly defined with only a single deuterium label; however, synthetic labeling of other ring positions is being pursued. ^{2}H NMR investigation of the backbone conformation in the dodecamer labeled at the 5′/5″ position, as well as ^{31}P investigations, is in progress. Solid-state NMR studies of base conformation in aberrant DNA sequences (bent) are also being pursued, along with the selective enrichment of base sites with other labels such as ^{13}C and ^{15}N.

Acknowledgments

We thank Dr. Paul Ellis, Dr. Regitze Vold, and Dr. Robert Vold for providing original copies of the simulation program MXQET. We also thank Brian Reid and Peter Flynn for assistance and computational access in the analysis of the dodecamer structure and Dr. W.-C. Huang for use of the 2″-labeled sample.

Registry No. d(CGCGAATTCGCG), 77889-82-8.

References

Abragam, A. (1961) in *Principles of Nuclear Magnetism*, pp 216–263, Oxford University Press, New York.

Alam, T. M., & Drobny, G. (1990a) *Biochemistry 29*, 3421–3430.

Alam, T. M., & Drobny, G. (1990b) *J. Chem. Phys. 92*, 6840–6846.

Arnott, S., & Hukins, D. W. L. (1972) *Biochem. Biophys. Res. Commun. 47*, 1504–1510.

Arnott, S., Campbell Smith, P. J., & Chandrasekharan, R. (1975) Nucleic Acids, in *CRC Handbook of Biochemistry and Molecular Biology*, Vol. 2, pp 411–422, CRC Press, Cleveland, OH.

Bax, A., & Lerner, L. (1988) *J. Magn. Reson. 79*, 429–438.

Bendel, P., Boesch, J., & James, T. L. (1983) *Biochim. Biophys. Acta 759*, 205–213.

Brandes, R., Vold, R. R., Vold, R. L., & Kearns, D. R. (1986) *Biochemistry 25*, 7744–7751.

Brandes, R., Vold, R. R., & Kearns, D. R. (1988a) *J. Mol. Biol. 202*, 321–332.

Brandes, R., Kearns, D. R., & Rupprecht, A. (1988b) *Biopolymers 27*, 717–732.

Brenneman, M. T., & Cross, T. A. (1990) *J. Chem. Phys. 92*, 1483–1494.

Cornell, B. A., Separovic, F., Baldassi, A. J., & Smith, R. (1988) *Biophys. J. 53*, 67–76.

Cross, T. A., & Opella, S. J. (1985) *J. Mol. Biol. 182*, 367–381.

Cross, T. A., Tsang, P., & Opella, S. J. (1983) *Biochemistry 22*, 721–726.

Dickerson, R. E. (1983) *J. Mol. Biol. 166*, 419–441.

Dickerson, R. E., & Drew, H. R. (1981) *J. Mol. Biol. 149*, 761–786.

DiVerdi, J. A., & Opella, S. J. (1981) *J. Mol. Biol. 149*, 307–311.

Fratini, A. V., Kopka, M. L., Drew, H. R., & Dickerson, R. E. (1982) *J. Biol. Chem. 257*, 14686–14707.

Greenfield, M. S., Ronemus, A. D., Vold, R. L., & Vold, R. R. (1987) *J. Magn. Reson. 72*, 89–107.

Griffin, R. G. (1981) *Methods Enzymol. 72*, 108–174.

Hiyama, Y., Roy, S., Cohen, J. S., & Torchia, D. A. (1989) *J. Am. Chem. Soc. 111*, 8609–8613.

Huang, W.-C., Orban, J., Kintanar, A., Reid, B. R., & Drobny, G. P. (1990) *J. Am. Chem. Soc.* (in press).

Iizuka, E. (1977) *Polym. J. 9*, 173–180.

Iizuka, E. (1978) *Polym. J. 10*, 235–237.

Iizuka, E. (1983) *Polym. J. 15*, 525–535.

James, T. L., Bendel, P., James, J. L., Keepers, J. M., Kollman, P. A., Lapidot, A., Murphy-Boesch, J., & Taylor, J. E. (1983) in *Nucleic Acids: The Vector of Life* (Pullman, B., & Jortner, J., Eds.) pp 155–167, Reidel Publishing, Dordrecht, Holland.

Kintanar, A., Alam, T. M., Huang, W.-C., Schindele, D. C., Wemmer, D. E., & Drobny, G. (1988) *J. Am. Chem. Soc. 110*, 6367–6372.

Kintanar, A., Huang, W.-C., Schindele, D. C., Wemmer, D. E., & Drobny, G. (1989) *Biochemistry 28*, 282-293.
Kopka, M. L., Frantini, A. V., Drew, H. R., & Dickerson, R. E. (1983) *J. Mol. Biol. 163*, 129-146.
Luz, Z., Poupko, R., & Samulski, E. T. (1981) *J. Chem. Phys. 74*, 5825-5837.
Nall, B. T., Rothwell, W. P., Waugh, J. S., & Rupprecht, A. (1981) *Biochemistry 20*, 1881-1887.
Nerdal, W., Hare, D. R., & Reid, B. R. (1989) *Biochemistry 28*, 10008-10021.
Nicholson, L. K., Moll, F., Mixon, T. E., LoGrasso, P. V., Lay, J. C., & Cross, T. A. (1987) *Biochemistry 26*, 6621-6626.
Privé, G. G., Heinemann, U., Chandrasegaran, S., Kan, L.-S., Kopka, M. L., & Dickerson, R. E. (1987) *Science 238*, 498-503.
Reid, B. R. (1987) *Q. Rev. Biophys. 20*, 1-34.
Rill, R. L. (1986) *Proc. Natl. Acad Sci. U.S.A. 83*, 342-346.
Rill, R. L., Hilliard, P. R., & Levy, G. C. (1983) *J. Biol. Chem. 258*, 250-256.
Robinson, C. (1961) *Tetrahedron 13*, 219-234.
Roy, S., Hiyama, Y., Torchia, D. A., & Cohen, J. S. (1986) *J. Am. Chem. Soc. 108*, 1675-1678.
Saenger, W. (1984) in *Principles of Nucleic Acid Structure*, Springer-Verlag, New York.
Santos, R. A., Tang, P., & Harbison, G. S. (1989) *Biochemistry 28*, 9372-9378.
Shindo, H., Fujiwara, T., Akustu, H., Matsumoto, U., & Kyogoku, Y. (1985) *Biochemistry 24*, 887-895.
Shindo, H., Hiyama, Y., Roy, S., Cohen, J. S., & Torchia, D. A. (1987) *Bull. Chem. Soc. Jpn. 60*, 1631-1640.
Stewart, P. L., Valentine, K. G., & Opella, S. J. (1987) *J. Magn. Reson. 71*, 45-61.
Tsang, P., Vold, R. R., & Vold, R. L. (1987) *J. Magn. Reson. 71*, 276-282.
Vold, R. R., Brandes, R., Tsang, P., Kearns, D. R., & Vold, R. L. (1986) *J. Am Chem. Soc. 108*, 302-303.
Wing, R., Drew, H., Takano, T., Broka, C., Tanaka, S., Itakura, K., & Dickerson, R. E. (1980) *Nature 287*, 755-758.

Resonance Raman Spectroscopic Characterization of Compound III of Lignin Peroxidase†

Muthusamy Mylrajan,‡ Khadar Valli, Hiroyuki Wariishi, Michael H. Gold,* and Thomas M. Loehr*
Department of Chemical and Biological Sciences, Oregon Graduate Institute of Science and Technology, 19600 N.W. von Neumann Drive, Beaverton, Oregon 97006-1999
Received May 4, 1990; Revised Manuscript Received July 9, 1990

ABSTRACT: Resonance Raman (RR) spectra of several compounds III of lignin peroxidase (LiP) have been measured at 90 K with Soret and visible excitation wavelengths. The samples include LiPIIIa (or oxyLiP) prepared by oxygenation of the ferrous enzyme, LiPIIIb generated by reaction of the native ferric enzyme with superoxide, LiPIIIc prepared from native LiP plus H_2O_2 followed by removal of excess peroxide with catalase, and LiPIII* made by addition of excess H_2O_2 to the native enzyme. The RR spectra of these four products appear to be similar and, thus, indicate that the environments of these hexacoordinate, low-spin ferriheme species must also be very similar. Nonetheless, the Soret absorption band of LiPIII* is red-shifted by 5 nm from the 414-nm maximum common to LiPIIIa, -b, and -c [Wariishi, H., & Gold, M. H. (1990) *J. Biol. Chem. 265*, 2070-2077]. Analysis of the iron-porphyrin vibrational frequencies indicates that the electronic structures for the various compounds III are consistent with an $Fe^{III}O_2^{\bullet -}$ formulation. The spectral changes observed between the oxygenated complex and the ferrous heme of lignin peroxidase are similar to those between oxymyoglobin and deoxymyoglobin. The contraction in the core sizes in compound III relative to the native peroxidase is analyzed and compared with that of other heme systems. EPR spectra confirm that the high-spin ferric form of the native enzyme, with an apparent $g = 5.83$, is converted into the EPR-silent LiPIII* upon addition of excess H_2O_2. Its magnetic behavior may be explained by antiferromagnetic coupling between the low-spin Fe^{III} and the superoxide ligand. The Fe–O_2 stretching vibration of the oxygenated peroxidase is observed at 563 cm^{-1} and shifts to 538 cm^{-1} with ^{18}O isotope. The Fe–histidine stretching vibration is observed at 245 cm^{-1} in ferrous peroxidase and appears to shift to 276 cm^{-1} in the oxygenated complex.

Phanerochaete chrysosporium, a white rot basidiomycete, is capable of degrading lignin, a heterogeneous phenylpropanoid polymer comprising 15-25% of woody plant cell walls (Gold et al., 1989; Kirk & Farrell, 1987; Buswell & Odier, 1987). Under secondary metabolic growth conditions, this fungus secretes two extracellular, H_2O_2-dependent heme enzymes, lignin peroxidase (LiP)[1] and manganese peroxidase (MnP), that are involved in lignin degradation (Gold et al., 1989; Kirk & Farrell, 1987; Buswell & Odier, 1987). LiP has

† This research was supported by grants from the National Institutes of Health (GM 18865 and GM 34468 to T.M.L.), the National Science Foundation (DMB 8904358 to M.H.G.), and the U.S. Department of Energy (DE-FG-06-87ER13715 to M.H.G.). The support of the NIH is further acknowledged for awards through its Biomedical Research Support Grant (S07 RR 07184) and Shared Instrumentation Grant (S10 RR 01482 and S10 RR 02676) programs used toward the purchase of research instrumentation used in this work.
* To whom correspondence should be addressed.
‡ Visiting Postdoctoral Research Associate from the Indian Institute of Technology, Madras 600036, India.

[1] Abbreviations: LiP, lignin peroxidase; LiPIII, lignin peroxidase compound III; CCP, cytochrome *c* peroxidase; DHF, dihydroxyfumarate; EPR, electron paramagnetic resonance; HRP, horseradish peroxidase; Im, imidazole; LPO, lactoperoxidase; MnP, manganese peroxidase; oxyHb, oxyhemoglobin; oxyLiP, same as LiPIIIa; oxyMb, oxymyoglobin; PP, protoporphyrin; RR, resonance Raman; RZ, Reinheitszahl = A_{407}/A_{280}.

0006-2960/90/0429-9617$02.50/0